SCINTILLATION SCREEN INVESTIGATIONS FOR HIGH CURRENT ION BEAMS AT GSI LINAC

E. Gütlich, P. Forck, R. Haseitl, P. Kowina
Gesellschaft für Schwerionenforschung GSI, Darmstadt, Germany

Abstract

Scintillation screens are widely used for qualitative beam profile monitoring. However, precise measurements might yield ambivalent results, especially for high beam currents. We have investigated the optical properties of various scintillating materials with different beams in the energy range 5.5 to 11.4 MeV/u delivered by the heavy ion linac at GSI. Investigations were not only focused on well-known sensitive scinitillators but also on ceramic materials with lower light yield. Their properties (yield, beam width, higher statistical moments) were compared to different quartz glasses. The image of each macropulse was recorded by a digital CCD camera and individually evaluated. For some materials, a decrease of the light yield occurs. For a focused beam, the imaged width depends on the material. Moreover, the light yield and width depend significantly on the screen temperature, which is increased by beam impact.

DEMANDS AND SETUP

For decades, scintillation screens have been used for beam profile measurement in nearly all accelerator facilities. These screens are an essential part of a pepper-pot ermittance system used for the determination of the width of "beamlets" created by a plate with ≈100 small holes. The realization at GSI, as used for high current operation of UNILAC, is described in [1]. The angular distribution within the phase space is calculated from the intensity distribution of the beamlets. This requires an accurate measurement of the spot's light distribution. However, there had been doubts concerning the accuracy of the pepper-pot method [2], which might be related to possible image deformation by the scintillating screen.

We investigated the optical properties of 16 fluorescence materials with ∞5.5 and 11.4 MeV/u and different beam currents as delivered by UNILAC. Typical sizes for the focused beam were σ≈2mm. Sensitive scintillation screens, like YAG:Ce or ZnS:Ag were irradiated in addition with lower currents. Ceramic materials with less light yield, like BN, ZrO_2, ZrO_2 doped with Mg, pure Al_2O_3 and Al_2O_3 doped with Cr (Chromox) were investigated and compared to quartz-glass (Herasil 102) and quartz-glass doped with Ce (M382); see Table 1.

A movable target ladder, as shown in Fig.1, was equipped with 6 different screens of ∅30mm and installed in a vacuum chamber. The irradiations were performed with pressure of ≈5×10^{-7} mbar. The target ladder allows beam observations without longer interruption, which ensures the same beam properties for all materials. The scintillation was observed by a digital CCD camera (AVT-Marlin) equipped with a monochrome chip of VGA resolution. A Pentax B2514ER lens system of 25 mm focal length equipped with a remote controlled iris was used for compensation of material dependent light yield. Moreover, the camera's inherent amplification was changed by the gain setting. The calculation of the light yield corrects both settings. The reproduction scale for the beam image was 10 pixel/mm. Data transmission was performed by the camera's Firewire interface to a high performance data acquisition system, [3] which enables the storage of an image from each macropulse for individual offline analysis.

Table 1: Compilation of investigated materials

Type	Material	Supplier
Crystal Scintillator	YAG:Ce, BGO, $CdWO_4$, CaF_2:Eu	Saint Gobain Crystals
Powder	ZnS:Ag	HLW
Ceramics	ZrO_2(Z700 20 A), ZrO_2:Mg (Z507), BN, Al_2O_3 and Al_2O_3:Cr (Chromox)	BCE Special Ceramics
Quartz-glass	Pure: Herasil 102, Ce doped: M382	Heraeus Quartz-glass

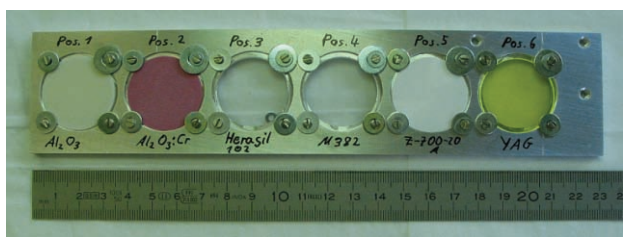

Figure 1: The target ladder equipped with ∅30mm screens is shown. The screen materials prior to irradiation are from left: pure Al_2O_3, Al_2O_3:Cr, Herasil, Quartz:Ce, ZrO_2 and YAG:Ce.

TYPICAL RESULTS AND ANALYSIS

The original beam image (an example is shown in Fig. 2 top) was projected to the beam's horizontal and vertical plane. A quantitative analysis was performed with the projection. In this work we show the horizontal projection but comparable results were obtained for the vertical direction. Two examples of such projections are shown in Fig. 2 bottom. For both displayed materials the total light yield decreases during irradiation. The shape of the peak is preserved for ZrO_2:Mg (shown left). For Al_2O_3 (shown right) the shape is modified mainly around the maximum;

this behavior is reflected by a broader width σ of about 11%. A typical increase of ≈10% corresponds to 0.2 mm, which is too small to be detected by a SEM-Grid, and is of minor importance in case of regular beam alignment. However, for the pepper-pot method it results in an over estimation of the emittance value. For the characterization of the distribution $p_i(x_i)$ not only the centre μ (1st moment) and standard deviation σ (2nd moment) were used, but also the skewness γ (3rd moment), describing the asymmetry and the kurtosis κ (4th moment), describing the peakedness of the distribution as given by:

Skewness: $$\gamma = \frac{1}{\sum p_i} \cdot \sum p_i \cdot \left(\frac{x_i - \mu}{\sigma} \right)^3$$

Kurtosis: $$\kappa = -3 + \frac{1}{\sum p_i} \cdot \sum p_i \cdot \left(\frac{x_i - \mu}{\sigma} \right)^4$$

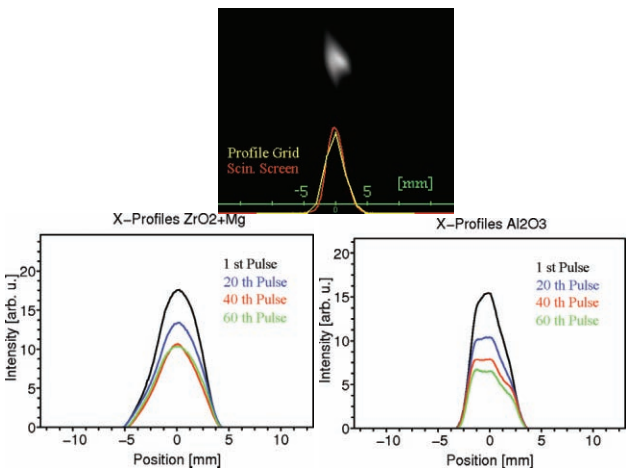

Figure 2: Examples of an original beam image (top) and the projection for ZrO_2:Mg (left) and Al_2O_3 (right) targets irradiated by 40 μA U^{28+} at 11.4 MeV/u. The variation from the 1st to 60th pulse for ZrO_2:Mg is width σ=1.78mm → 1.83mm, and kurtosis κ=-0.50 → -0.61. For Al_2O_3 the variation is significant: σ=1.30mm → 1.45mm and κ=-0.66 → -0.88.

SURFACE MODIFICATION

In Fig. 3 an example is shown for the irradiation with a high current 11.4 MeV/u Ar-beam of about $4x10^{10}$ particles per pulse (ppp), which corresponds to 0.7 mA and a 100 μs long pulse. The light yield of the BN screen decreased within the 1800 macro-pulses where as the beam width increased significantly caused by an irreversible damage of the screen. As expected from investigations of BN at CERN [4], the initially white surface became grey. Comparable surface modifications were observed for most ceramic materials with the least changes for ZrO_2:Mg. However, these modifications do not necessarily imply a lower light yield. In particular, ZrO_2 showed a very fast surface modification without significant decrease of the yield; this result confirms the finding in [4]. By baking ZrO_2 to 250^0C over 4 hours, this modification was reversible. The investigated quartz-glass Herasil showed no visible, permanent surface modification.

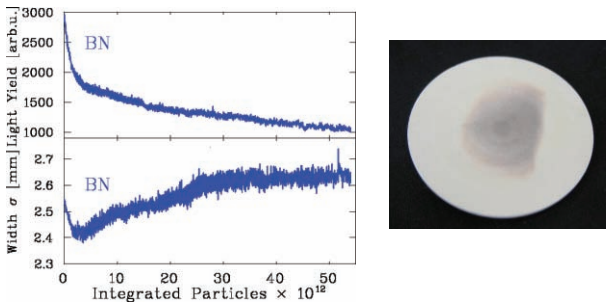

Figure 3: Left: Light yield and beam width σ for BN target irradiated by 1800 macropulses of ≈$4x10^{10}$ ppp Ar^{10+} at 11.4 MeV/u. Right: The ∅30mm BN screen after irradiation.

MEDIUM CURRENT INVESTIGATIONS

For a medium current of 30 μA and 100 μs delivery of Ar^{10+} beam at 11.4 MeV/u, the light yield and the beam width for different materials are compared in Fig. 4. As expected, the investigated materials have up to two orders of magnitude different light yield (integrated over 100 μs beam delivery) with Al_2O_3:Cr being the most and ZrO_2 the least sensitive material. This is consistent with a measurement reported by CERN [5]. The light yield was nearly constant during the irradiation for all materials. However, the determined beam width differed in a reproducible manner between the materials: For the given beam parameters, Herasil showed 22 % less width than ZrO_2:Mg. For three materials (BN, Al_2O_3:Cr and ZrO_2) the same width was recorded. As depicted in Fig. 5, the shape of the distribution differed for the materials, as rep resented by the relative peakedness. (The centre and the skewness were the same for all materials within the statistical fluctuations.) The described behaviour was reproduced with other ion beams of comparable parameters.

The average beam power for the parameters of Fig. 4 was 150 mW, resulting in an average temperature of 47^0 C on the backside of the ZrO_2:Mg screen as determined by aPT100 thermo-element. The peak power was 1.5 kW. Temperature effects will be discussed later on.

Presently, the reason for the different width reading is not well understood; it might be attributed to saturation effects or self-absorption. The different values of the kurtosis could help to clarify this topic. A more positive value is expected if absorption dominates, while a more negative value should occur for saturation. Moreover, a diffuse refraction at the surface and within the bulk material could contribute to a broadening. For ceramics it could be more pronounced due to the finite grain size. A laser-based method described in [5] let us estimate a spatial resolution for Al_2O_3:Cr ceramics to be ≈100 μm (compared to 50 μm for YAG:Ce and 35 μm for CsI, respectively). Since in all cases previously untreated materials were used, the broadening cannot be attributed to

any surface degradation caused by the beam, as discussed above for Fig. 3.

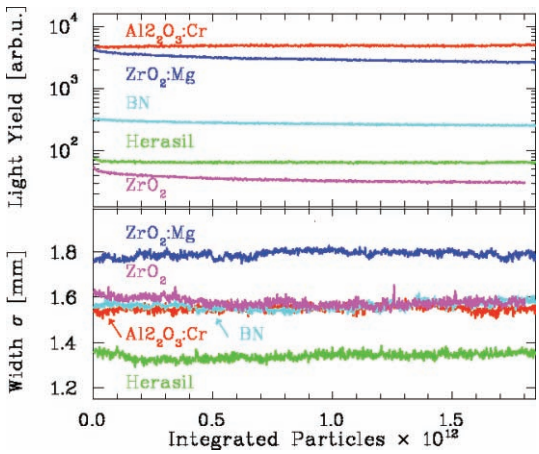

Figure 4: Light yield and beam width for different materials irradiated by 1000 macro-pulses of 1 Hz repetition rate with ≈2x10^9 ppp Ar^{10+} at 11.4 MeV/u.

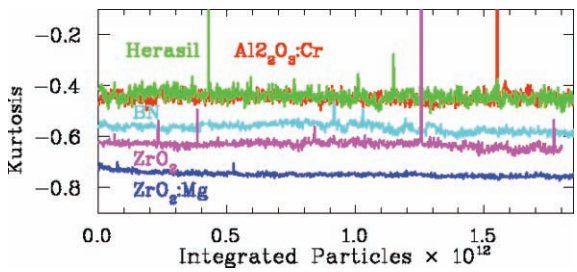

Figure 5: Kurtosis for the beam parameters of Fig. 4.

HIGH CURRENT INVESTIGATIONS

The interest of pepper-pot emittance measurements arises from the UNILAC high current operation with several mA. An example for high current measurement is shown in Fig. 6, where the screens were irradiated by Ar^{10+} with a current of 310 µA within 100 µs delivery time corresponding to 2x10^{10} ppp. The peak power was ≈14 kW while the average power was 3.8 W. As expected the light yield of the various materials differed of several orders of magnitude. In contrary to the medium current measurement of Fig. 4, the yield of ZrO_2:Mg relative to the other materials is lower.

For the four materials Quartz:Ce, ZrO_2:Mg, BN and Herasil the yields dropped significantly during the irradiation. The determined image widths vary within a factor of 2. The variation is larger as compared to the medium current measurement. A light yield decrease coincides with a smaller image width reading, but with a slightly different time constant. Since it was expected that the yield reduction is correlated with the screen temperature, a break in the beam delivery of 3 min was scheduled to let the screens relax to the original room temperature. For Herasil and ZrO_2:Mg the light yield and the beam width showed reproducible time behaviour and reached a constant value. BN suffered from permanent surface modification, as discussed for Fig. 3, while for Quartz:Ce the light yield is permanently reduced without visible surface modification. For Al_2O_3 the yield was constant whereas for Al_2O_3:Cr the yield even increased. In both cases, a broadening of the image width occurred in a reproducible manner.

For all materials, the reading of the beam centre and skewness was constant.

Using a PT100 thermo-element at the backside of ZrO_2:Mg screen the average temperature of 240^0 C was determined for comparable beam parameters with an average power of 2.3 W (compared to 3.8 W for the measurement of Fig. 6). However, the front-side temperature during 100 µs beam delivery was much higher due the ion range of about 20 to 170 µm (depending on the ion species and target density).

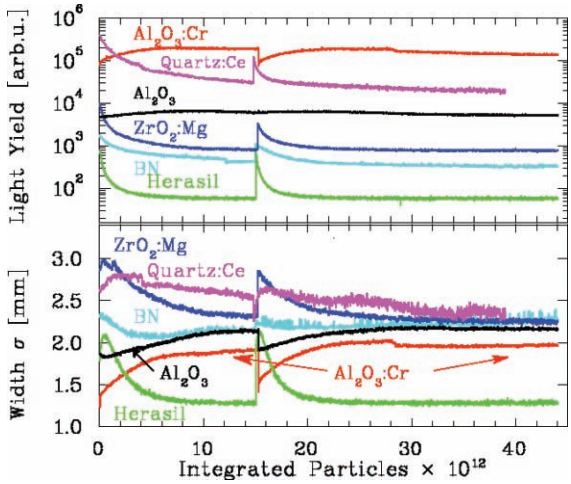

Figure 6: Light yield and beam width for different materials irradiated by 2200 macro-pulses of 2.6 Hz repetition rate with ≈2x10^{10} ppp Ar^{10+} at 11.4 MeV/u. After 5 min of irradiation, a 3 min break was introduced for relaxation to room temperature, followed by 10 min irradiation.

The interpretation of the temperature behaviour is difficult: As reviewed in [6,7] the light yield of scintillators depends significantly on temperature. For commonly used scintillators (like NaI:Tl, BGO, $CdWO_4$) the yield decreases as a function of temperature. It is related to a higher probability of non-radiative transitions from the upper scintillating levels competing with the fluorescence decay. Presently, we are lacking a detailed knowledge of these properties for the investigated materials. Moreover, the behaviour of the image width for Herasil and ZrO_2:Mg can be qualitatively described by the fact that the material is significantly stronger heated at the beam centre as compared to the beam edges. This results in a dominant decrease of the light yield at the peak area. After a certain (material dependent) irradiation time, a steady-state temperature distribution is reached, leading to a constant yield and width reading.

For Al_2O_3:Cr the yield increases with temperature. It might be related to an increased excitation probability from trapped states of the lattice (as it is the basis of thermo-luminescence). For BN and Quartz:Ce the discussed irreversible decrease of the light yield seems to dominate. Due to the different temperature dependent physical processes for the various materials, it does not astonish that the equilibrium width reading differs. For a quantitative interpretation, a detailed model is required, taking thermal diffusion, emissivity and temperature dependent light yield into account.

To investigate the temperature dependences, variable breaks between the irradiation were introduced to allow cooling to room temperature. As depicted in Fig. 7 for Herasil and ZrO_2:Mg, the length of the break did not influence the time constant for the yield reduction, equilibrium value, or width reading. It also proved the reproducibility for those materials.

LOW CURRENT INVESTIGATIONS

For comparison the properties of well known'scintillators under low current irradiation were investigated. In Fig. 8 the results are shown for the 17 nA C^{2+} beam of 100 µs length and 12.6 Hz repetition rate. The average power was 0.6 mW and the peak power 1.1 W. The yield of the materials differs by one order of magnitude, with YAG:Ce being a very efficient scintillator. However, even for these materials, quite different image widths were recorded. BGO showed the smallest value; YAG:Ce, $CdWO_4$ and CaF_2:Eu gave a ≈25% larger reading. This is remarkable, because YAG:Ce is frequently used for low current beam profile measurements. The powder ZnS:Ag shows a significant decrease of the yield and width reading even for this low current irradiation with light ions, i.e., low energy deposition.

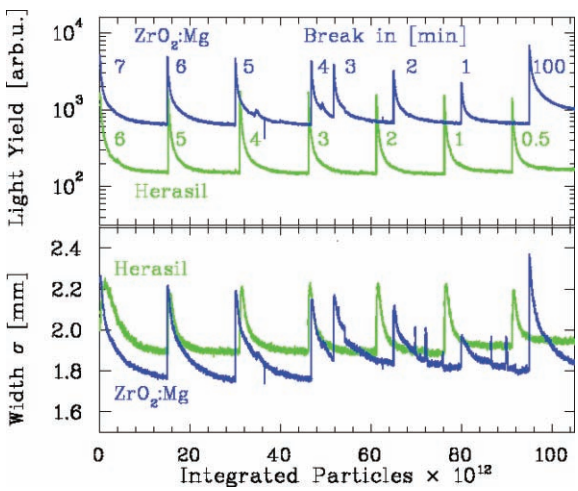

Figure 7: Light yield and beam width for ZrO_2:Mg and Herasil irradiated by 5500 macro-pulses of 2.4 Hz repetition rate with ≈$2.4x10^{10}$ ppp Ar^{10+} at 11.4 MeV/u; break durations are indicated. (The irradiation time varies.)

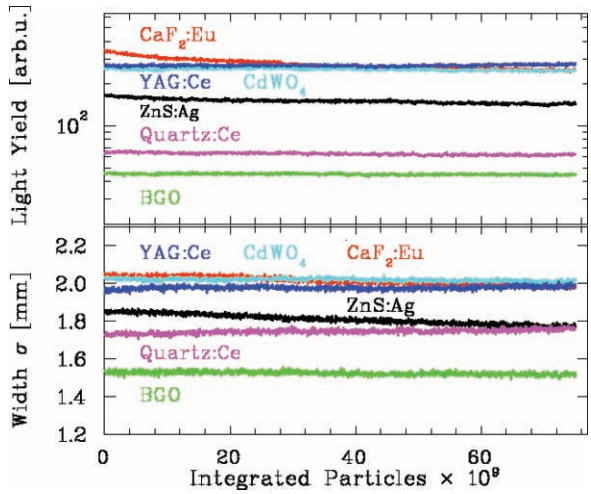

Figure 8: Light yield and beam width for different materials irradiated by 15000 macro-pulses of 12.6 Hz repetition rate with ≈$5x10^6$ ppp C^{2+} at 11.4 MeV/u. 10 macro-pulses are binned together.

CONCLUSION

Several scintillation materials were investigated under various beam conditions. Different readings of the image width for various materials were determined even for well known crystalline scintillators. The described behavior was reproducible under different beam conditions. Further data analysis is in progress to distinguish between saturation, diffuse refraction and self-absorbing of scintillation light. Statistical moments are considered for this purpose, but an interpretation might be difficult due to the presence of several effects. Additional beam-based tests are required to distinguish between these effects. For high current applications, the properties seem to be strongly dependent on the surface temperature, which is significantly increased during beam delivery. This knowledge is essential for choosing a well-suited material for the pepper-pot emittance device. Following the high current investigations at least BN and Quartz:Ce can't be used due to the permanent degradation. It seems that Herasil is a good candidate, because it shows a narrow image width and no significant surface modification even by high current irradiation. Being a transparent material, the diffuse reflections at the grain boundaries are avoided. However, its suitability has to be confirmed by ongoing beam-based investigations.

ACKNOWLEDGEMENT

We acknowledge the valuable discussion and practical support by T. Sieber and M. Frauenfeld from MPI-Kernphysik, Heidelberg. Moreover, we thank Z. Soares Macedo and G. C. Santana from University of Sergipe, Brazil for the supplier of several BGO ceramics [8].

REFERENCES

[1] T. Hoffmann et al., *Proc. Beam Instrum. Workshop Stanford*, p. 432 (2000).
[2] W. Barth, L. Groening, D. Liakin, *Proc. DIPAC03 Mainz,* p. 56 (2003).
[3] F. Becker et al., *GSI Scientific Report* 2007.
[4] C. Bal et al., *Proc. DIPAC05 Lyon*, p. 57 (2005).
[5] R. Jung, G. Ferioli., S. Hutchins, *Proc. DIPAC03 Mainz,* p. 10 (2003).
[6] G.F. Knoll, *Radiation Detection and Measurement*, John Wiley & Son, New York (1999).
[7] G. Blasse, B.C. Grabmaier, *Luminescence Materials,* Springer Verlag (1994).
[8] G. C. Santana, *J. Mater. Sci*. 42:2231 (2007).